

# Simultaneous optimization of stiffeners' layout and of composite laminate properties on a stiffened composite space launcher skirt

F. Savine<sup>1,2</sup>, F.X. Irisarri<sup>1</sup>, C. Julien<sup>1</sup>, A. Vincenti<sup>2</sup>, Y. Guerin<sup>3</sup>

<sup>1</sup> DMAS, ONERA, Université Paris Saclay, {florent.savine, francois-xavier.irisarri, cedric.julin}@onera.fr

<sup>2</sup> Sorbonne Université, CNRS, UMR 7190, Institut d'Alembert, angela.vincenti@sorbonne-universite.fr

<sup>3</sup> CNES, Direction des lanceurs, yannick.guerin@cnes.fr

---

**Résumé** — Combining the high stiffness-to-mass ratio of both stiffened structures and of composite materials, as well as their capacity of tailoring the local stiffness properties of a structure can contribute to further lighten already highly optimized space-launcher structures. In the present work, a component-based topological optimization method, which is aimed to design stiffening paths, is coupled with a bi-level optimization approach of composite laminates. This enables the optimization of the stiffening paths (number, location and geometry of stiffeners) simultaneously with the material and thickness properties of composite laminates, demonstrating a significant gain in structural performances compared to a metallic stiffened structure of equivalent mass.

**Mots clés** — Stiffener layout optimization, component-based method, bi-level optimization of composite laminates, polar formalism.

---

## 1 Introduction

Primary structures in space launcher applications are currently designed using either metallic rib-stiffened solutions (FIGURE 1) or composite sandwich structures. These designs are light and efficient in sustaining compressive and bending loads on cylindrical or conical parts with length-to-diameter ratios close to unity, which is the typical aspect ratio of space launcher components. Combining the use of composite materials with rib-stiffened reinforcements could contribute to further reduce the mass of these structures.

To achieve such designs, the main challenge is to conjointly optimize the stiffening layout (number, location, path and cross-section geometry of the stiffeners) as well as the layups of the constitutive composite materials of skins and stiffeners. As of today, few have tackled the problem [1, 5]. Most of the available methods either focus on the optimization of the composite stacks while restricting the possible stiffener locations to pre-determined patterns (linear, grid, stringer-frame) [8, 3], or they explore innovative stiffening paths, similarly to topological optimization, with limited possibilities on material optimization [6, 9].

The present work proposes an optimization method capable of simultaneously designing the stiffening geometry (number, size, location and path of stiffeners), not restricted to predefined patterns, as well as the composite laminates composing the skin of the structure.

In the following, we describe the approaches adopted in this work to model the stiffening geometry (component-based strategy, Section 2) and the distribution of anisotropic elastic properties of the constitutive materials, based on the polar formalism (Section 3). We then explain how these approaches are integrated into the simultaneous optimization process (Section 4) and we finally show cases of application and results (Section 5).

## 2 Modeling stiffeners for layout optimization

In order to build the finite-element model of the stiffening structure for analysis, a geometrical representation of the stiffeners (position, layout, size) is projected onto a ground structure of beam elements, as illustrated in FIGURE 2.



FIGURE 1 – Example of a metallic stiffened structure : the Intertank Structure (ITS) of the Lower Liquid Propulsion Module (LLPM) on the Ariane 6 launcher [2]

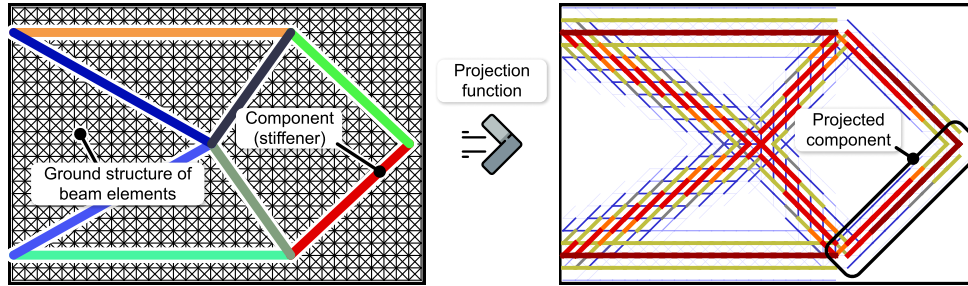


FIGURE 2 – Left : Overlay of the geometrical model of the components (colored segments) onto a ground structure of beam elements (background black network) used for the projection. Right : resulting structural model of the stiffeners, as issued from the projection.

The major idea is to approximate a stiffener, defined at the component level by its length and cross-sectional properties, using a set of beam elements from the ground structure. FIGURE 2 highlights one component (left side : red segment, representing one stiffener) and the corresponding projection over the ground structure of beam elements (right side, in the square-box : projected component, i.e. set of beams with associated cross-sectional properties corresponding to the highlighted red component). Whenever the position, geometry and size of the component change, the set of beams within the ground structure is updated accordingly by modifying the cross-sectional properties of the beam elements. The principle of the projection is that beam elements which are close and well aligned to the component have assigned higher values of cross-sectional properties, whilst the cross-sectional properties decrease when getting far from the component. Hence, the mesh remains fixed while the component may move and rotate freely on the surface.

In order to select the set of beam elements from the ground structure for the structural representation of the stiffener, "projection functions" are used, which establish the updated values of the cross-sectional properties of the beam elements as a fraction of the cross-sectional properties of the component. The result of the projection is an updated structural model, which is ready for finite-element analysis (see FIGURE 2). The projections functions  $\phi^{(P)}$  establish the cross-sectional properties  $P = \{A, I_y, I_z, J, h\}$  (area, inertia, etc. ) of the beam elements with respect to the corresponding cross-sectional properties  $P_c$  of the component as follows :

$$P = \phi^{(P)} \cdot P_c \quad (1)$$

Each projection function  $\phi^{(P)}$  is tailored for each property  $P$ , but they all share the same general form. Their values ranging between 0 and 1 are determined by the product of three filters :

$$\phi^{(P)} = f_a \cdot f_d^{(P)} \cdot f_l \quad (2)$$

where the  $f_i$  are filters written in the form of Gaussian functions :

- $f_a$  is an angle filter that cancels out the elements that are not closely aligned with the component ;
- $f_d^{(P)}$  is a distance filter that cancels out the elements that are distant from the stiffener ;

- $f_l$  is a location filter that cancels out elements that are not located within the two extremities of the component.

Whilst the angle filter  $f_a$  and the location filter  $f_l$  are the same for all cross-sectional properties, the distance filter  $f_d^{(P)}$  is adapted specifically for each property  $P$ . In order to build the FE structural model filter functions are evaluated for each beam element from the ground structure model as well as the resulting projection function (2), so that the cross-sectional properties of every beam element are set according to expression (1).

Finally, in order to accommodate more than one component on the surface, intersections and overlaps of components must be handled : for each component  $c$  ( $c \in \{1, \dots, N_c\}$ , where  $N_c$  is the overall number of components in the geometrical representation), one can evaluate the resulting projection functions  $\phi_c^{(P)}$  for all beam elements in the ground FE mesh. Then, one has to fix a rule for the definition of the final value of the projection function  $\phi^{(P)}$  for each beam element in order to build the structural representation of the stiffeners. The value of  $\phi^{(P)}$  of each beam element is determined by conserving the maximum components' contributions  $\phi_c^{(P)}$ . In the case of gradient-based optimization, the max function cannot be used directly as it is not differentiable. Consequently, it is approximated in this work by a  $p$ -norm :

$$\phi^{(P)} = \left[ \phi_{\min}^p + (1 - \phi_{\min}^p) \sum_{c=1}^{N_c} \left( \phi_c^{(P)} \right)^p \right]^{\frac{1}{p}} \quad (3)$$

where  $\phi_{\min}$  is introduced as a small positive lower bound to avoid an ill-posed analysis, as done in [8]. FIGURE 2 shows an example of application of the projection function in the case of several components over one single plate (left side of the figure) and the resulting projected finite-element beam model (right side of the figure).

This method has been successfully implemented in a gradient-based optimization process [4] : the first and more straightforward application concerns the case of fixed material properties and corresponds to the results on the metallic case (isotropic material) presented in this paper, SECTION 5. In the following, we explain how the optimization approach of stiffening layout can be coupled to the optimization of the constitutive composite material properties.

### 3 Modeling laminates for layup optimization

The general problem of optimizing a stacking sequence with respect to an objective  $F$  and  $i$  constraints  $g_i$  can be formulated as follows :

$$\begin{aligned} \min_{\{\theta, n\}} \quad & F \\ \text{w.r.t.} \quad & \theta = [\theta_1, \dots, \theta_n] \in [-90; 90]^n \\ & g_i \leq 0 \end{aligned} \quad (4)$$

where  $\theta = [\theta_1, \dots, \theta_n]$  is the sequence of orientations of the  $n$  plies. The singular characteristic of this problem is that the number of plies is itself a variable of the optimization, thus the total number of variables of the problem is variable with  $n$ . Furthermore, it is highly non-linear and non-convex.

The bi-level framework constitutes an efficient way of solving this problem. It is based on the dual representations of a laminate, either by its stacking sequence or by its homogeneous material properties in membrane  $\mathbf{A}$ , bending  $\mathbf{D}$  and membrane-bending coupling  $\mathbf{B}$ , related together via the Classical Laminate Plate Theory (CLPT). The principle consists in dividing the optimization of the stacking sequence into two distinct problems, chained one after the other :

- the first-level problem aims at optimizing the material properties  $\mathbf{A}, \mathbf{B}, \mathbf{D}$  and the thickness  $t$  of the homogeneous material representing a laminate, with respect to the objective and constraints of the global optimization problem (4).
- the second-level problem aims at identifying a stacking sequence  $[\theta_1, \dots, \theta_n]$  that corresponds to the target material properties and thickness issued from the first-level problem.

This work focuses on the first-level optimization problem, formulated as :

$$\begin{aligned} \min_{\{A,B,D,t\}} \quad & F \\ \text{w.r.t.} \quad & \{A, B, D\} \in \mathcal{D}_{\text{lam}} \\ & t \in \mathcal{D}_{\text{thick}} \\ & g_i \leq 0 \end{aligned} \quad (5)$$

where  $F$  and  $g_i$  are optimization objective and constraint functions. Optimization variables are the laminate thickness  $t$ , varying within a given range  $\mathcal{D}_{\text{thick}}$  of admissible values, as well as the elastic properties  $A$ ,  $B$  and  $D$  of the laminate, varying within an admissible domain  $\mathcal{D}_{\text{lam}}$ . The optimal solution constitutes target material properties  $A_T$ ,  $B_T$  and  $D_T$  and target thickness  $t_T$  for the second-level problem. The advantage of this formulation is that the space of the mechanical properties is more regular and convex than the space of the stacking sequences. Hence gradient-based algorithms are used as solvers, which allows to limit the number of calls to finite-elements analysis and thus the computational costs. Furthermore, the number of variables is independent of the number of plies therefore simplifying thickness variations.

However, the usual representation of the  $A$ ,  $B$ ,  $D$  matrices by their Cartesian components is not a convenient parametrization : since  $A$ ,  $B$ ,  $D$  characterize an anisotropic material, their terms are intrinsically related and depend on the orientation of the material with respect to the frame of reference. Hence a more efficient parametrization of the first-level optimization consists in using the polar representation, that allows to characterize any planar tensor of the elasticity type by 6 independent polar parameters [3] :  $T_0$ ,  $T_1$  characterize the isotropic part,  $R_0$ ,  $R_1$  characterize the anisotropic part and  $\phi_0$ ,  $\phi_1$  are angles characterizing the orientation of the anisotropic components.

In addition, assumptions on the laminate relative to common design constraints allow to simplify the design problem. The laminate is assumed to be made of identical plies, making  $T_0$  and  $T_1$  independent of the stacking sequence and equal to those of the base ply material. The laminate is also assumed to be quasi-homogeneous (uncoupled  $B = O$  and homogeneous membrane-bending behavior  $A^* = D^*$ ) and orthotropic, which is simply expressed in the polar formalism as :

$$\phi_0 - \phi_1 = K \frac{\pi}{4}, \quad K \in \{0, 1\} \quad (6)$$

These assumptions reduce to only three the total number of variables necessary to optimize the laminate properties, out of the 18 originally :  $R_{0k} = (-1)^K R_0$ ,  $R_1$  and  $\phi_1$ , for both membrane and bending behaviors. Finally, the admissible values of polar parameters are restricted by the so-called geometrical bounds, that determine the domain of existence  $\mathcal{D}_{\text{lam}}$  of all orthotropic laminates :

$$[\rho_{0k}, \rho_1, \phi_1] \in \mathcal{D}_{\text{lam}} = \begin{cases} \rho_{0k} \in [-1; 1] \\ \rho_1 \in [0; 1] \\ \phi_1 \in ]-\pi/2; \pi/2] \\ \Gamma = 2\rho_1^2 - 1 - \rho_{0k} \leq 0 \end{cases} \quad (7)$$

where  $\rho_{0k}$ ,  $\rho_1$  are respectively the  $R_{0k}$  and  $R_1$  values normalized by the corresponding base-ply values,  $R_{0k}^{\text{ply}}$  and  $R_1^{\text{ply}}$ .

Finally, a variable change is defined in order to remove the need for the inequality constraint  $\Gamma$  in (7), by mapping the  $(\rho_{0k}, \rho_1)$ -domain onto a rectangular  $(\alpha, \beta)$ -domain :

$$\begin{cases} \rho_{0k} = \beta(2\alpha^2 - 1 - \rho_{0k_{\max}}) + \rho_{0k_{\max}} \\ \rho_1 = \alpha\beta \end{cases} \quad \text{where} \quad \begin{cases} \alpha \in \left[0; \sqrt{\frac{\rho_{0k_{\max}} + 1}{2}}\right] \\ \beta \in [0, 1] \end{cases} \quad (8)$$

where  $\rho_{0k_{\max}}$  is a user defined upper-bound of the variable  $\rho_{0k}$ .

Such parametrization based on the polar formalism can be applied in either cases of uniform elastic properties over the structure (constant stiffness laminates) or non-uniform properties (variable stiffness laminates) : in this latter case, variables  $\rho_{0k}$ ,  $\rho_1$  (or their counterparts  $\alpha, \beta$ ) and  $\phi_1$  are defined for each zone or element of the structure.

## 4 Simultaneous optimization process

The method developed in SECTION 3 to solve the stiffener layout optimization problem is now combined with the first-level problem of the laminate optimization of SECTION 4. The latter is generalized into a variable-stiffness composite skin design by dividing the skin into  $N_z$  zones, each having assigned three material variables ( $\rho_{0k}$ ,  $\rho_1$  and  $\phi_1$ ) and one thickness variable  $t$  :

$$\begin{aligned} \min_{\{\mathbf{X}, \Xi, \mathbf{T}\}} \quad & F \\ \text{w.r.t.} \quad & \mathbf{X} \in \mathcal{D}_{\text{skin}} \\ & \Xi \in \mathcal{D}_{\text{lam}} \\ & \mathbf{T} \in \mathcal{D}_{\text{thick}} \\ & g_i \leq 0 \end{aligned} \quad (9)$$

where  $F$  and  $g_i$  are the objective and constraint functions, the vector of coordinates  $\mathbf{X}$  defines the positions of extremities of the components within the geometrical domain  $\mathcal{D}_{\text{skin}}$  of the structure,  $\Xi$  and  $\mathbf{T}$  are respectively the vectors of the polar parameters and of the thickness for each zone of the skin, varying respectively in the domains  $\mathcal{D}_{\text{lam}}$  and  $\mathcal{D}_{\text{thick}}$ . In order to avoid abrupt variations of thickness and material variables between contiguous zones, a filtering strategy is implemented.

The optimization problem is then solved using a gradient-based algorithm. The optimization process is illustrated in FIGURE 3. After an initialization of the design variables defining the geometry of the component model, the thicknesses and the material properties of the composite skin, the components are projected on the structural model at each iteration  $j$  via the projection functions and the properties of the shell elements of the ground FE model are updated. A structural analysis outputs the values of the objective and constraint functions. The Method of Moving Asymptotes (MMA) [7] is used to calculate the values of the design variables for the iteration  $j + 1$ . The optimization process stops when either a maximum number of iterations  $j_{\text{max}}$  is attained, or a stagnation criterion on the maximum change of the design variables values from iterations  $j - 1$  to  $j$  is fulfilled.

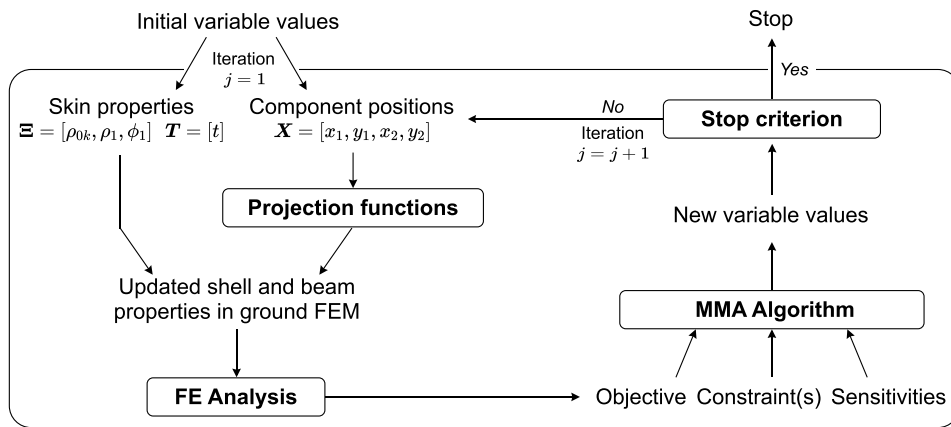


FIGURE 3 – Schematic overview of the simultaneous optimization of the stiffener layout and of the material and thickness properties of the skin

## 5 Application

This application aims to assess the benefits of using composite materials rather than metallic structures and how the simultaneous optimization of the material properties and component layout influences the optimal solution.

### 5.1 Test case

The case of study consists in solving the optimization problem (9) of minimal compliance for the simplified model of a 0/1 interstage launcher skirt presented in FIGURE 4, considering constraints  $g_i$  on

the mass, buckling critical load and stress flux through the structure :

$$g_i = \begin{cases} M_T < M_{T0} \\ \max(N_x) < N_0 \\ \min(N_x) > N_0 \\ \lambda_i > \lambda_0, i \in \{1, \dots, 20\} \end{cases} \quad (10)$$

where  $M_{T0} = 12.55$  kg constrains the overall mass of the interstage skirt (IS) skin and of the components  $M_T$ ,  $N_0 = 550$  kN constrains the flux  $N_x$  at the top perimeter of the junction skirt and  $\lambda_0 = 2.4$  constrains the buckling coefficients of the first 20 modes  $\lambda_{1\dots 20}$ .

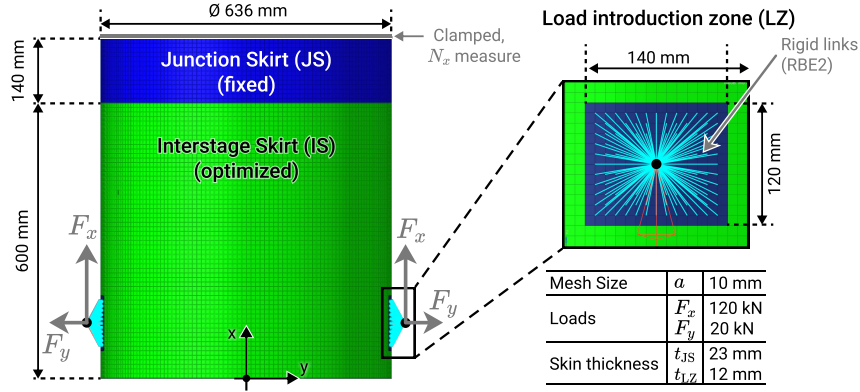


FIGURE 4 – Simplified model of a 0/1 interstage skirt

Three optimization cases are led considering the IS skin made of either one of the following materials :

- aluminum (uniform and fixed material properties) : optimization variables are  $\mathbf{X}$  (stiffening path) and shell thickness  $\mathbf{T}$  ;
- isotropic composite material (uniform material properties) : optimization variables are  $\mathbf{X}$  (stiffening path) and shell thickness  $\mathbf{T}$  ;
- anisotropic composite material (variable stiffness laminates) : optimization variables are  $\mathbf{X}$  (stiffening path), shell thickness  $\mathbf{T}$  and anisotropic polar parameters  $\mathbf{\Xi}$ , restricted to the domain of orthotropic quasi-homogeneous laminates.

Their properties are given in TABLE 1. The components are either made of aluminum for the aluminum skin or of ‘black aluminum’ (properties in 1) for both the isotropic and anisotropic skins.

Material	$E_1$ (GPa)	$E_2$ (GPa)	$G_{12}$ (GPa)	$\nu_{12}$	$\rho$ (kg.m <sup>-3</sup> )
Aluminum	70.81	70.81	26.62	0.33	2800
Isotropic composite	69.68	69.68	26.88	0.30	1600
Composite base-ply	181	10.3	7.17	0.28	1600

TABLE 1 – Material properties

## 5.2 Results

The response values of the feasible minimum compliance design for each case are presented in TABLE 2 (the mass constraint is active and satisfied in all cases). The results show a significant reduction of compliance when using an isotropic composite material compared to aluminum. Furthermore the margin to the buckling constraint is also significantly increased. The difference of performance can directly be explained by the higher specific modulus of composites, which allows to use a greater volume of material for the same mass as a metallic structure. As FIGURE 5 illustrates, the number of components and the overall thickness of the skin is greater in the isotropic case. However, the thickest zones and the components are located in the same areas of the structure.

The optimization of the anisotropy of the skin further reduces the compliance of the model while increasing the margin to buckling. The distributions of material properties in FIGURE 6 reveal highly

Material	$C/C_0$	$\lambda_1/\lambda_0$	$N_x/N_0$	Best/Total It.
Aluminum	$C_0$ (204 J)	1.02	[-1.01;0.68]	86/ 95
Isotropic composite	0.61	2.61	[-0.99;0.71]	83/114
Anisotropic composite	0.40	4.33	[-0.99;0.70]	147/153

TABLE 2 – Feasible minimum compliance solutions considering different materials for the skin of the model. The components are either in aluminum (for the aluminum skin) or in isotropic composite (for both the isotropic and anisotropic skins.)

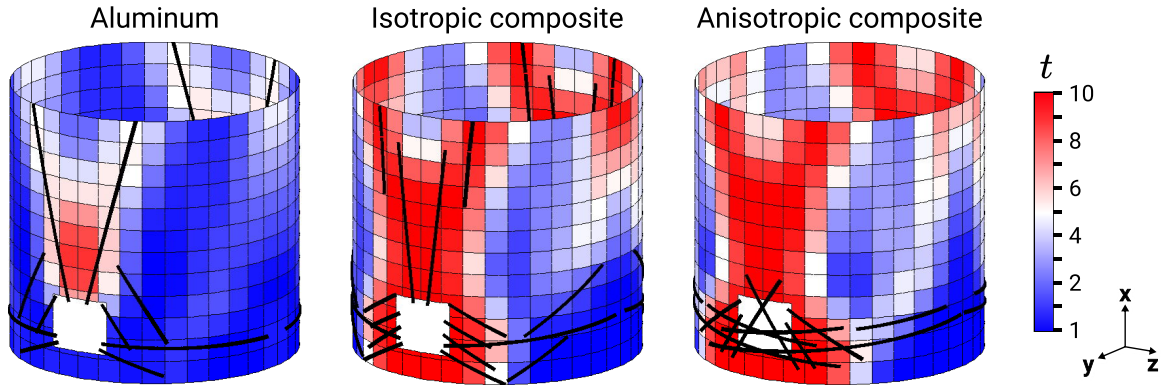


FIGURE 5 – Thickness distribution and component placement of the feasible minimum compliance solutions considering different materials for the skin of the model. The fields of the material variables for the anisotropic case are described in FIGURE 6.

oriented material properties in the critical zones of the models. The extra reinforcement that was initially provided by components in the isotropic case is thus here ensured by the material properties. Components can thus be used to stiffen other locations on the cylinder, hence explaining a different distribution of the components and the better performance of the structure. This highlights the dependency between the stiffer locations and the material properties and supports the benefit of optimizing them both simultaneously.

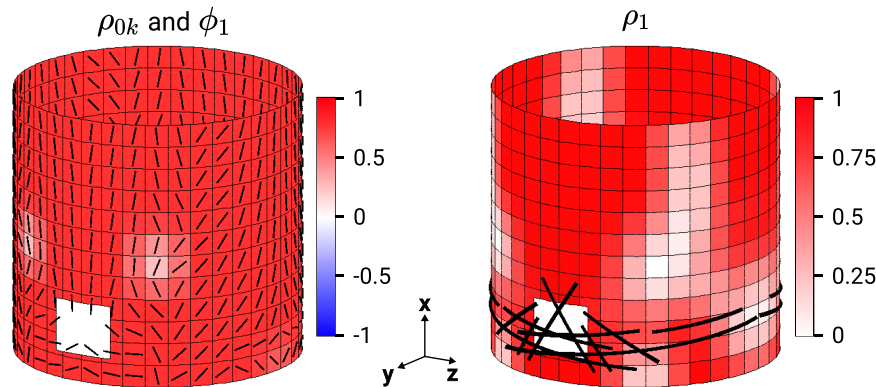


FIGURE 6 – Fields of the material variables for the feasible minimum compliance design with an anisotropic material.

## Références

- [1] A. Alhajahmad. *Minimum weight design of curvilinearly grid-stiffened variable-stiffness composite fuselage panels considering buckling and manufacturing constraints* Thin-Walled Structures, 1-17, 2021.
- [2] J. Merino, A. Patzelt, A. Steinacher, M. Windisch, G. Heinrich, R. Forster, C. Bauer. *Ariane 6 - Tanks and structures for the new european launcher*, Deutscher Luft- und Raumfahrtkongress , 450255 :1-10, 2017

- [3] M. Montemurro, A. Vincenti, P. Vannucci. *A Two-Level Procedure for the Global Optimum Design of Composite Modular Structures—Application to the Design of an Aircraft Wing-Part1*, Journal of Optimization Theory and Applications, 155(1), 1-23, 2012.
- [4] F. Savine, F.-X. Irisarri, C. Julien, A. Vincenti, Y. Guerin. *A component-based method for the optimization of stiffener layout on large cylindrical rib-stiffened shell structures*, Structural and Multidisciplinary Optimization, 64(4), 1843-1861, 2021.
- [5] K. Singh, R. K. Kapania. *Buckling Load Maximization of Curvilinearly Stiffened Tow-Steered Laminates*, Journal of Aircraft, 56(6), 1-13, 2019.
- [6] Z. Sun, R. Cui, T. Cui, C. Liu, S. Shi, X. Guo. *An Optimization Approach for Stiffener Layout of Composite Stiffened Panels Based on Moving Morphable Components (MMCs)*. Acta Mechanica Solida Sinica 33, 650-662, 2020.
- [7] K. Svanberg. *The method of moving asymptotes—a new method for structural optimization*, International Journal for Numerical Methods in Engineering, 24(2), 359-373, 1987.
- [8] W. Wang, S. Guo, N. Chang, W. Yang. *Optimum buckling design of composite stiffened panels using ant colony algorithm*, Composite Structures, 92(3), 712-719, 2010.
- [9] S. Zhang, J. A. Norato, A. L. Gain, N. Lyu. *A geometry projection method for the topology optimization of plate structures*, Structural and Multidisciplinary Optimization, 54(5), 1173-1190, 2016.